Time between milestone events in the Alzheimer's disease amyloid cascade

Philip S. Insel, MS[1,2],*, Michael C. Donohue, PhD[3], David Berron, PhD[1], Oskar Hansson, MD, PhD[1,4], Niklas Mattsson-Carlgren, MD, PhD[1,5,6]

[1]Clinical Memory Research Unit, Department of Clinical Sciences Malmö, Lund University, Sweden

[2]Department of Psychiatry, University of California, San Francisco, CA, USA

[3]Alzheimer's Therapeutic Research Institute, Keck School of Medicine, University of Southern California, San Diego, CA, USA

[4]Memory Clinic, Skåne University Hospital, Malmö, Sweden

[5]Department of Neurology, Skåne University Hospital, Lund, Sweden

[6]Wallenberg Center for Molecular Medicine, Lund University, Lund, Sweden

*Corresponding authors: Philip Insel and Niklas Mattsson-Carlgren, Clinical Memory Research Unit, Department of Clinical Sciences Malmö, Lund University, Sweden

Phone: (Philip Insel) +1 858 652 8480. E-mail: philip.insel@med.lu.se, niklas.mattsson@med.lu.se

Search terms: (1) Alzheimer's disease, (2) β-amyloid, (3) tau PET, (4) cognition

Abstract

Objective: Estimate the time-course of the spread of key pathological markers and the onset of cognitive dysfunction in Alzheimer's disease.

Methods: In a cohort of 336 older adults, ranging in cognitive functioning, we estimated the time of initial changes of Aβ, tau, and decreases in cognition with respect to the time of Aβ-positivity.

Results: Small effect sizes of change in CSF Aβ42 and regional Aβ PET were estimated to occur several decades before Aβ-positivity. Increases in CSF tau occurred 11-12 years before Aβ-positivity. Temporoparietal tau PET showed increases 4-5 years before Aβ-positivity. Subtle cognitive dysfunction was observed 7-9 years before Aβ-positivity.

Conclusions: Increases in tau and cognitive dysfunction occur years before the presence of significant Aβ. Explicit estimates of the time for these events provide a clearer picture of the time course of the amyloid cascade and identify potential windows for specific treatments.

Introduction

Disconcerting clinical trial results for the treatment of Alzheimer's disease (AD) have led to a shift toward earlier intervention, focusing on the early clinical or presymptomatic phases, when biomarkers are needed to identify the disease. The amyloid cascade (Hardy and Selkoe, 2002) is thought to start with elevated levels of two key amyloids in the brain, β-amyloid (Aβ) and tau, and end with severe cognitive and functional impairment (Jack et al., 2010). Growing evidence suggests that an early sign that the cascade has begun is change in cerebrospinal fluid (CSF) Aβ, potentially detectable prior to significant Aβ deposition in the brain as measured by positron emission tomography (PET) (Palmqvist et al., 2016). This accumulation of Aβ has been suggested to be followed by increases in CSF tau and the spread of tau pathology beyond the temporal lobe (Braak and Braak, 1991; Schöll et al., 2016). The build-up and spread of these two brain pathologies is paralleled by gradual cognitive and functional decline (Zetterberg and Mattsson, 2014).

Previous neuropathological and biomarker data suggest that the overall time course of AD is several decades (Li et al., 2017; Villemagne et al., 2013). In autosomal dominant AD, the estimated years to clinical onset has been used to estimate the time-course of different biomarkers in AD (Bateman et al., 2012). However, the time-course of the spread of Aβ and tau and the onset of clinical symptoms in sporadic AD is unknown. With repeated measures of Aβ over time, the level and rate of change with respect to the key initiating AD pathology may offer a measure of disease progression in sporadic AD. With level and change information, the time from the threshold for significant Aβ pathology can be estimated within individuals, providing the temporal disease

progression information important for evaluating biomarker trajectories. Without longitudinal information, cross-sectional studies frequently categorize subjects into two groups – those below a threshold for significant pathology and those above, where subjects just below the threshold who will cross over within months are considered pathologically equivalent to subjects who will not cross over for decades. By incorporating longitudinal information, disease progression with respect to Aβ pathology can be represented to reflect its continuous nature, resulting in a more powerful way to model the relationship between Aβ and downstream processes.

The aim of this study was to evaluate time-from-Aβ-positivity (TFAβ+) in sporadic AD. Using serial 18F-florbetapir (Aβ) PET measurements, rates of change of Aβ were estimated and used to calculate the time-from-threshold for each subject. These subject-specific estimates of the proximity to the threshold for Aβ-positivity (Aβ+) were then used to model the trajectories and temporal ordering of other key markers in AD including CSF Aβ42, regional Aβ PET, several measures of tau including CSF phosphorylated (P-tau) and total tau (T-tau), regional 18F-flortaucipir (AV-1451) tau PET, and cognition. Estimates of the time and ordering of these pathophysiological changes may facilitate the design of future prevention trials and identify a window for early treatment.

Materials and methods

Standard protocol approvals, registrations, and patient consents.

This study was approved by the Institutional Review Boards of all of the participating institutions. Informed written consent was obtained from all participants at each site.

Data Availability

All data is publicly available (http://adni.loni.usc.edu/).

Participants

Data were obtained from the Alzheimer's Disease Neuroimaging Initiative (ADNI) database (http://adni.loni.usc.edu/, www.adni-info.org) on 1/21/2020. An initial analysis was done on all ADNI participants with available Aβ PET data (in N=963 CU, Aβ+ MCI and Aβ+ AD), to facilitate the estimation of TFAβ+. The population in the primary analysis only included ADNI participants with measurements of both Aβ and tau PET. Of these, all cognitively unimpaired (CU), prodromal AD (Aβ+ MCI) and Aβ+ AD dementia participants were included in the analysis, where Aβ-positivity was defined using a previously established threshold (Standardized Uptake Value Ratio, SUVR = 1.10) (Joshi et al., 2012). Aβ- MCI (N=224, including Aβ- CU to MCI progressors) and Aβ- "AD dementia" subjects (N=51, including Aβ- MCI to AD dementia progressors; we consider these to be misdiagnosed, because we assume AD requires Aβ+) were not included in the main analysis given our aim to model disease progression over the AD continuum and not other diseases, but visualizations of their biomarker data are included

for comparison in Figures 2-4 (see Figure legends). Additional description is included in the statistical analysis section.

Cerebrospinal fluid biomarker concentrations

Cerebrospinal fluid (CSF) samples were collected at baseline by lumbar puncture in a subsample (N=185). CSF Aβ42, total tau (T-tau) and phosphorylated tau (P-tau) were measured by an xMAP assay (INNOBIA AlzBio3, Ghent, Belgium, Fujirebio), as described previously (Olsson et al., 2005; Shaw et al., 2009).

PET Imaging

Methods to acquire and process Aβ (18F-florbetapir) PET image data were described previously (Landau et al., 2012). We used an a priori defined threshold for Aβ-positivity (SUVR=1.1) (ADNI, 2012; Joshi et al., 2012) applied to the ratio of the average of the four target regions (temporal, cingulate, frontal, and parietal lobes) and the cerebellum, in the estimation of time-from-Aβ-positivity, described in detail below. In a second part of the analysis, five Aβ PET ROI outcomes were considered (Landau and Jagust, 2015; Mormino et al., 2009), (1) the temporal lobe (middle and superior temporal lobe), (2) the parietal lobe (precuneus, supramarginal, inferior and superior parietal lobe), (3) the cingulate gyrus (isthmus, posterior, caudal and rostral anterior cingulate), (4) the frontal lobe (pars opercularis, pars triangularis, pars orbitalis, caudal/rostral middle frontal, medial/lateral orbitofrontal, frontal pole, and superior frontal lobe), and (5) a composite of regions thought to be early in accumulating Aβ (precuneus and posterior

cingulate) (Palmqvist et al., 2017). 18F-florbetapir ROIs were expressed as SUVRs with a cerebellar reference region.

Methods to acquire and process tau (18F-flortaucipir) PET image data were described previously (Maass et al., 2017). Six tau ROI outcomes, corrected for partial-volume, were considered: (1) the medial temporal lobe (MTL) (amygdala, entorhinal and parahippocampal cortex), (2) the lateral temporal lobe (LTL) (inferior/middle/superior temporal lobe, banks of the superior temporal sulcus, transverse temporal lobe, temporal pole), (3) the medial parietal lobe (MPL) (isthmus cingulate, precuneus), (4) the lateral parietal lobe (LPL) (inferior/superior parietal lobe, supramarginal), (5) frontal lobe (pars, orbitofrontal and middle/superior frontal lobe), and (6) the occipital lobe (cuneus, lingual, pericalcarine, and lateral occipital lobe). 18F-flortaucipir ROIs were expressed as SUVRs with an inferior cerebellar grey matter reference region. Full details of PET acquisition and analysis can be found at http://adni.loni.usc.edu/methods/.

Cognition

Cognitive measures assessed included the Mini-Mental State Examination (MMSE) as a measure of global cognition, and the Preclinical Alzheimer's Cognitive Composite (PACC), as a measure of early AD-related cognitive changes. The PACC comprised the MMSE, the Logical Memory Delayed Word Recall from the Wechsler Memory Scale, the Alzheimer's Disease Assessment Scale—Cognitive Subscale Delayed Word Recall, and the Trail Making Test part B (log transformed) (Donohue et al., 2017, 2014).

Statistical Analysis

The aims of these analyses were to evaluate the relationship between the estimated TFAβ+ and CSF, PET, and cognitive responses. Because TFAβ+ was not directly observed, in a first step, linear mixed-effects models were fit to all available longitudinal global Aβ PET SUVR data to estimate subject-specific intercepts and slopes of Aβ pathology. Because Aβ slopes are unlikely to remain constant over long periods of time as subjects move toward and away from the Aβ threshold, natural splines (Hastie and Tibshirani, 1990) were used to estimate the nonlinear shape of the slopes with respect to baseline Aβ, using quantile regression. Rather than modeling the mean Aβ slope with respect to baseline Aβ, quantile regression provides a separate curve for each quantile, allowing the relationship between slope and intercept to differ depending on the location in the distribution of Aβ slope. For each subject, TFAβ+ was estimated by integrating over each subject's quantile curve between the subject's intercept and the threshold for Aβ-positivity (PET SUVR = 1.1). For example, for a subject with a baseline SUVR of 1.2 and a slope in the 0.6 quantile, TFAβ+ was taken to be the time it would take to go from SUVR = 1.1 to 1.2, using the slope estimates from the quantile curve. For incremental changes on the x-axis (baseline SUVR), the time required to travel the incremental distance is equal to distance/rate. Using the trapezoid rule (Atkinson, 1989), TFAβ+ is the sum of these incremental times spanning SUVR = 1.1 to 1.2. An example of calculating TFAβ+ is given in the top left panel of Figure 1.

To evaluate the accuracy of the TFAβ+ estimates, we compared the observed times of Aβ+ to the estimated times of Aβ+ values in participants who were Aβ- at baseline and became Aβ+ during follow-up. Observed time of Aβ+ occurred in the

interval between the last Aβ- scan and the first Aβ+ scan. The observed time was calculated as a weighted average of the two scan times, weighted proportionally toward the scan where the participant was closest to hitting the threshold. Observed and estimated values were compared in N=37 participants who crossed the threshold for Aβ+ and remained Aβ+ throughout follow-up.

Our analyses aim to model participants who are ostensibly on the AD trajectory and had calculable TFAβ+. Therefore, of the 963 participants with Aβ PET, we excluded N=16 participants with negative Aβ accumulation rates (negative rates were largely driven by one early high Aβ PET measure), we also excluded N=6 participants with low levels of Aβ and accumulation rates such that they were predicted to become Aβ+ later than 120 years of age (biomarker data from these subjects are included for visual comparisons in Figures 2-4, see Figure legends). We included subjects where the TFAβ+ metric indicated very early accumulation of Aβ, but for participants estimated to have become Aβ+ before age 40 (N=24, median estimated age at Aβ+ = 30, IQR: 24 to 34), we truncated TFAβ+ to age 40, based on previously described rates of Aβ-positivity in middle age (Jansen et al., 2015).

In the second step, the relationship between TFAβ+ and the responses was modeled using monotone penalized regression splines. Generalized cross-validation was used to tune the smoothing parameter (Wood, 1994). Cognitive responses were covaried for age, gender and education; CSF Aβ42, T-tau, P-tau and PET measures were covaried for age and gender.

In order to account for the uncertainty across steps 1 and 2, the entire process was repeated in 500 bootstrap samples to estimate 95% confidence intervals for the association between TFAβ+ and the responses.

Meaningful effect sizes of change of increase in pathology or decrease in cognition with respect to TFAβ+ were estimated. A Cohen's d effect size of 0.2 SD was considered small, 0.5 SD was considered medium, and a 0.8 SD effect was considered large (Cohen, 1988). A 0.2 standard deviation (SD) change from the mean response at the longest times (least pathological) from Aβ-positivity was taken to be the initial point of meaningful change. A 0.5 SD change was also shown as a more substantial effect size of change. We also estimated change, 95% confidence intervals, and statistical significance of change for each response at TFAβ+ = 0, the time of Aβ-positivity, with bootstrap-estimated standard errors.

Baseline associations between demographics and TFAβ+ were assessed using Spearman correlation for age and education and the Wilcoxon rank-sum test for gender. Associations between diagnosis and demographics were assessed using Wilcoxon rank-sum test for continuous variables and Fisher's Exact test for categorical variables. All analyses were done in R v3.5.1 (www.r-project.org).

Results

Cohort Characteristics

Two-hundred and twenty-eight CU (128 Aβ- and 100 Aβ+), 70 Aβ+ MCI and 38 Aβ+ AD participants were included in the analysis. The diagnostic groups varied by mean age (CU-, 70.1 years old [SD=5.8]; CU+, 72.9 years old [SD=6.6]; MCI, 72.0 years old [SD=6.9]; AD, 74.5 years old [SD=7.2]; p<0.001). The diagnostic groups varied by sex (CU-, 60.2% female; CU+, 58.0% female; MCI, 41.4% female; AD, 47.4% female; p=0.05). The groups differed by mean years of education (CU-, 16.7 years [SD=2.4]; CU+, 16.9 years [SD=2.3]; MCI, 16.0 years [SD=2.5]; AD, 15.6 years [SD=2.5]; p=0.007). The groups varied by proportion of *APOE* ε4+ (CU-, 25.4%; CU+, 50.5%; MCI, 60.9%; AD, 54.3%; p<0.001).

Aβ PET and Estimation of TFAβ+

TFAβ+ was estimated with a median of 3 (range: 1 to 5) Aβ PET scans per participant. The average time between first and last scan was 3.3 years (SD=2.9) and the average time between scans was 2.2 years (SD=0.8). Across diagnoses, TFAβ+ ranged from -35.9 to 47.0 years, where higher (positive) TFAβ+ values indicate more time spent with a significant Aβ burden. The average TFAβ+ was -9.3 years (SD=6.9) for CU-, 13.9 years (SD=11.2) for CU+, 21.1 years (11.7) for MCI, and 25.8 years (11.0) for AD participants (p<0.001, comparing CU+, MCI, and AD only). TFAβ+ was highly correlated with observed time of Aβ+ (ρ=0.93, p<0.001, bottom left panel of Figure 1). Higher TFAβ+ was significantly associated with older age (ρ=0.30, p<0.001), lower

education (ρ=-0.15, p=0.01) and *APOE* ε4-positivity (mean TFAβ+ in *APOE* ε4- = 3.0 (SD=16.5) years and mean TFAβ+ in *APOE* ε4+ = 13.7 (SD=16.0) years, p<0.001). TFAβ+ was not associated with sex (mean TFAβ+ = 9.5 (SD=17.4) and 6.6 (SD=16.8) in males and females, respectively, p=0.13). Within-diagnosis TFAβ+ distributions are shown on the bottom right panel of Figure 1. Quantile curves of the relationship between Aβ intercepts and slopes are also shown in the top right panel of Figure 1, displaying the variation of acceleration of Aβ deposition over different levels of baseline Aβ.

Regional Aβ PET

Five regional ROIs (precuneus + posterior cingulate, frontal lobe, cingulate gyrus, temporal and parietal lobes) are shown plotted against TFAβ+ in Figure 2. All 5 regions were estimated to reach a small, but meaningful (0.2 SD) increase in SUVR between 16-17 years before Aβ-positivity, i.e. TFAβ+ = 0. Effect sizes over the span of TFAβ+ are shown in Figure 2. At TFAβ+ = 0, all regions showed large, significant increases in SUVR (ΔSUVR ≥ 0.13, p≤0.01) with the precuneus + posterior cingulate composite showing the largest increase (ΔSUVR = 0.19, p < 0.01) and the temporal lobe showing the smallest (ΔSUVR = 0.13, p < 0.01). Effect sizes for all regions were large (>1) by the time of Aβ+. Table 1 summarizes the values of the responses at the longest times before Aβ+, i.e. the least pathological TFAβ+. Table 1 also shows the value and change of each response at the time of Aβ-positivity (TFAβ+ = 0), p-value and corresponding 95% confidence interval, the effect size of change of each response, and the 0.2 SD change point with respect to TFAβ+.

CSF

CSF responses are plotted against TFAβ+ in Figure 3. A 0.2 SD drop in CSF Aβ42 was estimated to occur 35 years before Aβ-positivity (TFAβ+ = -35). At TFAβ+ = 0, CSF Aβ42 showed a very large effect size (ΔAβ42 = -74 ng/L, p<0.01, effect size = -2.17). At TFAβ+ = -2, or two years before Aβ-positivity, the population curve passes through a previously published CSF Aβ42 threshold for Aβ-positivity (192 ng/L) (Shaw et al., 2009).

A 0.2 SD increase in CSF T-tau and P-tau was estimated to occur 11-12 years before the time of Aβ-positivity (TFAβ+ = -12 and -11, respectively). At TFAβ+ = 0, significant increases of medium effect size of T-tau (ΔT-tau = 25 ng/L, p=0.01, effect size = 0.59) and P-tau (ΔP-tau = 14 ng/L, p=0.02, effect size = 0.55) were observed.

Tau PET

Six regional ROIs (MTL, LTL, MPL, LPL, frontal and occipital lobes) are shown plotted against TFAβ+ in Figure 4. Five of the six regions were estimated to reach a 0.2 SD increase in SUVR 3-5 years before Aβ-positivity, with the occipital lobe reaching a 0.2 SD increase one year after Aβ-positivity. Effect sizes over the span of TFAβ+ are shown in Figure 4. At TFAβ+ = 0, four regions (MTL, LTL, MPL, LPL) showed significant small increases in SUVR (ΔSUVR ≥ 0.12, p≤0.05) with the MTL showing the largest effect size (0.35). The frontal and occipital lobes did not increase significantly by TFAβ+ = 0 (ΔSUVR = 0.09, 0.07, respectively, p=0.13). Estimates are summarized in Table 1.

Cognition

Cognitive measures are shown in Figure 5. The MMSE showed a 0.2 SD drop

nine years before Aβ-positivity, followed by the PACC seven years before Aβ-positivity.

Neither measure decreased significantly by the time of Aβ-positivity, although the PACC

was borderline (ΔMMSE = -0.80, p=0.17, effect size=-0.34; ΔPACC = -0.61, p=0.07,

effect size=-0.39). Summary curves and 0.2 SD change points are shown in Figure 6.

Discussion

Several biological processes develop over time in sporadic AD, including accumulation of Aβ and tau across wide areas of the brain, as well as cognitive decline. Based on the amyloid cascade hypothesis, a relevant overarching time scale of the disease processes could be based on the development of Aβ pathology (Koscik et al., 2020). We have therefore integrated Aβ PET level and rate of change information to place each individual on a pathological timeline. This timeline can then be used to estimate the time of downstream events in the amyloid cascade. We estimated several major milestone events of AD progression including a small drop in CSF Aβ42 35 years before Aβ-positivity and a small increase in regional Aβ PET deposition 17 years before Aβ-positivity. Using the biomarkers tested here, the first changes in CSF Aβ42 may define the onset of AD. Small increases in tau pathology were estimated to occur 11-12 years before Aβ-positivity, as measured by CSF and 5 years before, as measured by PET. More substantial and statistically significant increases in CSF as well as temporoparietal tau PET were detected by the time of Aβ-positivity. Small effects of cognitive dysfunction occurred 7-9 years before Aβ-positivity, coinciding with previous reports (Insel et al., 2017). These findings provide a general time scale for initial changes in sporadic AD, which may inform clinical trials aimed at specific stages of the disease.

A 0.2 SD difference, a small, but meaningful increase in levels of CSF tau and temporoparietal lobe tau are observed years before the current threshold for Aβ-positivity. In the context of secondary prevention trials where Aβ-positivity at current thresholds is required for study inclusion, tau levels in these participants would already

have been increasing for several years, likely more. The finding that temporoparietal tau starts to increase prior to other regions is in accordance with 18F-flortaucipir studies on other populations. Cross-sectional studies showed early tau deposition in cognitively healthy elderly (with or without significant Aβ pathology) in temporal and medial parietal regions, most dominant in entorhinal and parahippocampal cortex, the amygdala and inferior temporal cortex. Longitudinal studies further suggest that cognitively healthy elderly accumulate tau in the medial temporal and medial parietal lobe, while (Aβ positive) AD dementia patients increased in tau primarily in the frontal lobe (Harrison et al., 2018). The spread of tau beyond the MTL to the parietal lobe and other regions may be a critical milestone in the progression of AD. The early changes observed in the MPL in this study coincide with a recent report of the earliest tau deposition found in medial parietal regions (precuneus and isthmus cingulate) in autosomal dominant AD (Gordon et al., 2019). Considering that a 0.2 SD increase in MPL tau can potentially be detected several years before Aβ-positivity (Figure 4), these data support the use of primary prevention trials against Aβ where treatment is initiated years before the current threshold for Aβ-positivity, if treatment efficacy relies on early intervention, prior to the development of tau pathology.

The initial descent in cognitive performance is estimated to occur 7-9 years before becoming Aβ+ (Figure 5). Reduced cognitive performance has repeatedly been shown to be associated with elevated levels of Aβ (Baker et al., 2017; Donohue et al., 2017; Insel et al., 2017, 2016), even within the subthreshold range (Landau et al., 2018), in cognitively unimpaired individuals. The result that CSF tau measures started to change between regional Aβ and cognition in this study is in accordance with the theory that

cognitive impairment in AD is caused primarily by tau pathology. This is also in line with other recent studies which show that cognitive impairment is more strongly related to accumulation of tau than to Aβ (Ossenkoppele et al., 2019), and that both tau and Aβ appear necessary for cognitive decline (Sperling et al., 2019). The ordering of the responses coincides with the magnitude of the effect sizes at the time of Aβ-positivity (Table 1), suggesting that initial changes in the responses continue to change in parallel through to the time of Aβ-positivity, without any major differences in acceleration.

In their 2018 draft guidance, the FDA indicated that because it is highly desirable to intervene as early as possible in AD, it follows that patients with characteristic pathophysiologic changes of AD but no subjective complaint, functional impairment, or detectable abnormalities on sensitive neuropsychological measures are an important target for clinical trials (Food and Drug Administration, 2018). If the spread of tau to the lateral temporal and parietal lobes becomes a defining characteristic of pathophysiological change in AD, the window to intervene as early as possible may shift to years before the current threshold for Aβ-positivity. It is possible that early accelerations of tau may have contributed to recent failures of anti-Aβ treatments in phase III clinical trials on Aβ-positive patients (Egan et al., 2018; Honig et al., 2018). Although selecting subjects that are Aβ-positive ensures that only AD patients are included in trials, the use of conservative thresholds to define Aβ-positivity may bias trial populations toward individuals where tau pathology has already accumulated, causing downstream injuries independent of Aβ, reducing the efficacy of anti-Aβ treatments.

This study has several limitations. Tau PET data were available for only a subsample of the data, limiting comparisons to a small cross-section of the full ADNI

data set. More data, especially longitudinal data in participants in the earliest stages of Aβ

changes, will be required for more precise change point estimates. These analyses lack

the power and precision to place the temporal and parietal tau regions in a particular

order with confidence, but instead demonstrate that temporoparietal tau increases years

before Aβ-positivity. The ADNI CU, MCI and AD cohorts are also age matched. The AD

patients, on average, have dementia by age 75, while the participants in the CU cohort

who may eventually develop AD, are unlikely to do so for many years, possibly decades.

By design, these cohorts with age matched groups are therefore on systematically

different disease trajectories with respect to age. If earlier onset is associated with a more

aggressive form of the disease, then the AD cohort may have the most aggressive form

while the CU cohort, the least aggressive. If the developing Aβ pathology in the ADNI

CU- cohort represents a less aggressive disease process compared with a more typical

AD process, the estimates reported here could be conservative and biased toward later

time estimates for downstream events. The ADNI MCI cohort may represent a more

typical trajectory with respect to downstream events along the Aβ pathological timeline.

These differences in disease trajectories are apparent from the cohort estimates in Figures

2-5. Additionally, the change point estimates are influenced by both biological variation

and measurement error, which varies from marker to marker. Change points in measures

with high variability in the "normal" range and excess measurement error may require

additional biological change to detect, despite an earlier, real increase in pathology.

ADNI participants are highly educated on average, reducing generalizability to some

degree. The associations between increasing Aβ pathology and downstream changes,

including increased tau pathology reported here do not imply causality. It remains

unknown whether and to what degree downstream pathological changes can be directly attributed to the accumulation of Aβ. Only studies with experimental interventions against Aβ-pathology, with clear verification of target engagement, can be used to show causal relationships between Aβ-deposition and putative downstream events.

Longitudinal information is required to evaluate how quickly an individual's pathophysiological changes are occurring and to accurately characterize their disease trajectory. Analyses limited to a cross-sectional evaluation of Aβ status are naïve to the time spent with a significant Aβ burden. Incorporating longitudinal information facilitates the estimation of the time-course of downstream events such as the spread of tau and the onset of subtle cognitive dysfunction. As the technology to measure AD pathology becomes more cost effective and noninvasive, such as plasma measures of Aβ or tau (Janelidze et al., 2020; Mielke et al., 2018; Palmqvist et al., 2019; Schindler et al., 2019), longitudinal evaluations in the context of trial-ready cohorts may greatly improve early diagnosis and expedite the execution of clinical trials in early AD.

Acknowledgements

Competing Interests

Mr. Insel, Dr. Berron and Dr. Donohue report no competing interests.

Dr. Mattsson-Carlgren has been a consultant for ADNI.

Dr. Hansson has acquired research support (for the institution) from Roche, GE

Healthcare, Biogen, AVID Radiopharmaceuticals and Euroimmun. In the past 2 years, he

has received consultancy/speaker fees (paid to the institution) from Biogen and Roche.

References

ADNI. 2012. ADNI Commonly Used Tables. https://adni.loni.usc.edu/wp-content/uploads/2012/08/instruction-about-data.pdf

Atkinson KE. 1989. An Introduction to Numerical Analysis, 2nd ed. New York: John Wiley & Sons.

Baker JE, Lim YY, Pietrzak RH, Hassenstab J, Snyder PJ, Masters CL, Maruff P. 2017. Cognitive impairment and decline in cognitively normal older adults with high amyloid-β: A meta-analysis. *Alzheimer's Dement Diagnosis, Assess Dis Monit* **6**:108–121. doi:10.1016/j.dadm.2016.09.002

Bateman RJ, Xiong C, Benzinger TLS, Fagan AM, Goate A, Fox NC, Marcus DS, Cairns NJ, Xie X, Blazey TM, Holtzman DM, Santacruz A, Buckles V, Oliver A, Moulder K, Aisen PS, Ghetti B, Klunk WE, McDade E, Martins RN, Masters CL, Mayeux R, Ringman JM, Rossor MN, Schofield PR, Sperling RA, Salloway S, Morris JC. 2012. Clinical and biomarker changes in dominantly inherited Alzheimer's disease. *N Engl J Med* **367**:795–804. doi:10.1056/NEJMoa1202753

Braak H, Braak E. 1991. Acta H ' pathologica Neuropathological stageing of Alzheimer-related changes. *Acta Neuropathol* **82**:239–259. doi:10.1007/BF00308809

Cohen J. 1988. Statistical Power Analysis for the Behavioral Sciences, 2nd ed. New York: Lawrence Earlbaum Associates.

Donohue MC, Sperling RA, Petersen R, Sun C-K, Weiner MW, Aisen PS. 2017. Association Between Elevated Brain Amyloid and Subsequent Cognitive Decline Among Cognitively Normal Persons. *JAMA* **317**:2305–2316. doi:10.1001/jama.2017.6669

Donohue MC, Sperling RA, Salmon DP, Rentz DM, Raman R, Thomas RG, Weiner M, Aisen PS, Australian Imaging, Biomarkers, and Lifestyle Flagship Study of Ageing, Alzheimer's Disease Neuroimaging Initiative, Alzheimer's Disease Cooperative Study. 2014. The preclinical Alzheimer cognitive composite: measuring amyloid-related decline. *JAMA Neurol* **71**:961–70. doi:10.1001/jamaneurol.2014.803

Egan MF, Kost J, Tariot PN, Aisen PS, Cummings JL, Vellas B, Furtek C, Harper Mozley L, Mahoney E, Vandenberghe R, Mukai Y, Voss T, Mo Y, Sur C,

Michelson D. 2018. Randomized Trial of Verubecestat for Mild-to-Moderate Alzheimer's Disease. *N Engl J Med* **378**:1691–1703. doi:10.1056/nejmoa1706441

Food and Drug Administration. 2018. Early Alzheimer's disease: developing drugs for treatment guidance for industry.

Gordon BA, Blazey TM, Christensen J, Dincer A, Flores S, Keefe S, Chen C, Su Y, Mcdade EM, Wang G, Li Y, Hassenstab J, Aschenbrenner A, Hornbeck R, Jack CR, Ances BM, Berman SB, Brosch JR, Galasko D, Gauthier S, Lah JJ, Masellis M, Dyck CH Van, Mintun MA, Klein G, Ristic S, Cairns NJ, Marcus DS, Xiong C, Holtzman DM, Raichle ME, Morris JC, Bateman RJ, Benzinger TLS. 2019. Tau PET in autosomal dominant Alzheimer's disease: relationship with cognition, dementia and other biomarkers. *Brain A J Neurol* **142**:1063–1076. doi:10.1093/brain/awz019 BRAIN

Hardy J, Selkoe DJ. 2002. The amyloid hypothesis of Alzheimer's disease: progress and problems on the road to therapeutics. *Science* **297**:353–356. doi:10.1126/science.1072994

Harrison TM, La Joie R, Maass A, Baker SL, Swinnerton K, Fenton L, Mellinger TJ, Edwards L, Pham J, Miller BL, Rabinovici GD, Jagust WJ. 2018. Longitudinal tau accumulation and atrophy in aging and alzheimer disease. *Ann Neurol* **85**:229–240. doi:10.1002/ana.25406

Hastie TJ, Tibshirani RJ. 1990. Generalized Additive Models. *Monogr Stat Appl Probab*. doi:10.1016/j.csda.2010.05.004

Honig LS, Vellas B, Woodward M, Boada M, Bullock R, Borrie M, Hager K, Andreasen N, Scarpini E, Liu-Seifert H, Case M, Dean RA, Hake A, Sundell K, Poole Hoffmann V, Carlson C, Khanna R, Mintun M, DeMattos R, Selzler KJ, Siemers E. 2018. Trial of Solanezumab for Mild Dementia Due to Alzheimer's Disease. *N Engl J Med* **378**:321–330. doi:10.1056/NEJMoa1705971

Insel PS, Donohue MC, Mackin RS, Aisen PS, Hansson O, Weiner MW, Mattsson N. 2016. Cognitive and functional changes associated with Aβ pathology and the progression to mild cognitive impairment. *Neurobiol Aging* **48**:172–181. doi:10.1016/j.neurobiolaging.2016.08.017

Insel PS, Ossenkoppele R, Gessert D, Jagust W, Landau S, Hansson O, Weiner MW,

Mattsson N. 2017. Time to amyloid positivity and preclinical changes in brain metabolism, atrophy, and cognition: Evidence for emerging amyloid pathology in alzheimer's disease. *Front Neurosci* **11**:1–9. doi:10.3389/fnins.2017.00281

Jack CR, Knopman DS, Jagust WJ, Shaw LM, Aisen PS, Weiner MW, Petersen RC, Trojanowski JQ. 2010. Hypothetical model of dynamic biomarkers of the Alzheimer's pathological cascade. *Lancet Neurol* **9**:119–128. doi:10.1016/S1474-4422(09)70299-6

Janelidze S, Mattsson N, Palmqvist S, Smith R, Beach TG, Serrano GE, Chai X, Proctor NK, Eichenlaub U, Zetterberg H, Blennow K, Reiman EM, Stomrud E, Dage JL, Hansson O. 2020. Plasma P-tau181 in Alzheimer's disease: relationship to other biomarkers, differential diagnosis, and longitudinal progression to Alzheimer's dementia. *Nat Med* **26**:379–386. doi:10.1038/s41591-020-0755-1

Jansen WJ, Ossenkoppele R, Knol DL, Tijms BM, Scheltens P, Verhey FRJ, Visser PJ, Aalten P, Aarsland D, Alcolea D, Alexander M, Almdahl IS, Arnold SE, Baldeiras I, Barthel H, van Berckel BNM, Bibeau K, Blennow K, Brooks DJ, van Buchem MA, Camus V, Cavedo E, Chen K, Chetelat G, Cohen AD, Drzezga A, Engelborghs S, Fagan AM, Fladby T, Fleisher AS, van der Flier WM, Ford L, Förster S, Fortea J, Foskett N, Frederiksen KS, Freund-Levi Y, Frisoni GB, Froelich L, Gabryelewicz T, Gill KD, Gkatzima O, Gómez-Tortosa E, Gordon MF, Grimmer T, Hampel H, Hausner L, Hellwig S, Herukka S-K, Hildebrandt H, Ishihara L, Ivanoiu A, Jagust WJ, Johannsen P, Kandimalla R, Kapaki E, Klimkowicz-Mrowiec A, Klunk WE, Köhler S, Koglin N, Kornhuber J, Kramberger MG, Van Laere K, Landau SM, Lee DY, de Leon M, Lisetti V, Lleó A, Madsen K, Maier W, Marcusson J, Mattsson N, de Mendonça A, Meulenbroek O, Meyer PT, Mintun MA, Mok V, Molinuevo JL, Møllergård HM, Morris JC, Mroczko B, Van der Mussele S, Na DL, Newberg A, Nordberg A, Nordlund A, Novak GP, Paraskevas GP, Parnetti L, Perera G, Peters O, Popp J, Prabhakar S, Rabinovici GD, Ramakers IHGB, Rami L, Resende de Oliveira C, Rinne JO, Rodrigue KM, Rodríguez-Rodríguez E, Roe CM, Rot U, Rowe CC, Rüther E, Sabri O, Sanchez-Juan P, Santana I, Sarazin M, Schröder J, Schütte C, Seo SW, Soetewey F, Soininen H, Spiru L, Struyfs H, Teunissen CE, Tsolaki M, Vandenberghe R, Verbeek MM, Villemagne VL, Vos SJB, van Waalwijk van Doorn

LJC, Waldemar G, Wallin A, Wallin ÅK, Wiltfang J, Wolk DA, Zboch M, Zetterberg H. 2015. Prevalence of Cerebral Amyloid Pathology in Persons Without Dementia: A Meta-analysis. *Jama* **313**:1924–1938. doi:10.1001/jama.2015.4668

Joshi AD, Pontecorvo MJ, Clark CM, Carpenter AP, Jennings DL, Mintun MA, Adler LP, Burns JD, Saha K, Sadowsky CH, Kovnat KD, Lowrey MJ, Arora A, Seibyl JP, Skovronsky DM. 2012. Performance Characteristics of Amyloid PET with Florbetapir F 18 in Patients with Alzheimer's Disease and Cognitively Normal Subjects. *J Nucl Med* **53**:378–384. doi:10.2967/jnumed.111.090340

Koscik RL, Betthauser TJ, Jonaitis EM, Allison SL, Clark LR, Hermann BP, Cody KA, Engle JW, Barnhart TE, Stone CK, Chin NA, Carlsson CM, Asthana S, Christian BT, Johnson SC. 2020. Amyloid duration is associated with preclinical cognitive decline and tau PET. *Alzheimer's Dement Diagnosis, Assess Dis Monit* **12**:1–10. doi:10.1002/dad2.12007

Landau S, Jagust W. 2015. Florbetapir processing methods. https://adni.bitbucket.io/reference/docs/UCBERKELEYAV45/ADNI_AV45_Methods_JagustLab_06.25.15.pdf

Landau SM, Horng A, Jagust WJ. 2018. Memory decline accompanies subthreshold amyloid accumulation. *Neurology* 10.1212/WNL.0000000000005354. doi:10.1212/WNL.0000000000005354

Landau SM, Mintun MA, Joshi AD, Koeppe RA, Petersen RC, Aisen PS, Weiner MW, Jagust WJ. 2012. Amyloid deposition, hypometabolism, and longitudinal cognitive decline. *Ann Neurol* **72**:578–586. doi:10.1002/ana.23650

Li D, Iddi S, Thompson WK, Donohue MC. 2017. Bayesian latent time joint mixed effect models for multicohort longitudinal data. *Stat Methods Med Res* 1–11. doi:10.1177/0962280217737566

Maass A, Landau S, Horng A, Lockhart SN, Rabinovici GD, Jagust WJ, Baker SL, La Joie R. 2017. Comparison of multiple tau-PET measures as biomarkers in aging and Alzheimer's disease. *Neuroimage* **157**:448–463. doi:10.1016/j.neuroimage.2017.05.058

Mielke MM, Hagen CE, Xu J, Chai X, Vemuri P, Lowe VJ, Airey DC, Knopman DS, Roberts RO, Machulda MM, Jack CR, Petersen RC, Dage JL. 2018. Plasma

phospho-tau181 increases with Alzheimer's disease clinical severity and is associated with tau- and amyloid-positron emission tomography. *Alzheimer's Dement* **14**:989–997. doi:10.1016/j.jalz.2018.02.013

Mormino EC, Kluth JT, Madison CM, Rabinovici GD, Baker SL, Miller BL, Koeppe RA, Mathis CA, Weiner MW, Jagust WJ. 2009. Episodic memory loss is related to hippocampal-mediated β-amyloid deposition in elderly subjects. *Brain* **132**:1310–1323. doi:10.1093/brain/awn320

Olsson A, Vanderstichele H, Andreasen N, De Meyer G, Wallin A, Holmberg B, Rosengren L, Vanmechelen E, Blennow K. 2005. Simultaneous measurement of β-amyloid(1-42), total Tau, and phosphorylated Tau (Thr181) in cerebrospinal fluid by the xMAP technology. *Clin Chem* **51**:336–345. doi:10.1373/clinchem.2004.039347

Ossenkoppele R, Smith R, Ohlsson T, Strandberg O, Mattsson N, Insel PS, Palmqvist S, Hansson O. 2019. Associations between tau, Aβ, and cortical thickness with cognition in Alzheimer disease. *Neurology* **92**:e601–e612. doi:10.1212/wnl.0000000000006875

Palmqvist S, Janelidze S, Stomrud E, Zetterberg H, Karl J, Zink K, Bittner T, Mattsson N, Eichenlaub U, Blennow K, Hansson O. 2019. Performance of Fully Automated Plasma Assays as Screening Tests for Alzheimer Disease-Related β-Amyloid Status. *JAMA Neurol* **76**:1060–1069. doi:10.1001/jamaneurol.2019.1632

Palmqvist S, Mattsson N, Hansson O. 2016. Cerebrospinal fluid analysis detects cerebral amyloid-?? accumulation earlier than positron emission tomography. *Brain* **139**:1226–1236. doi:10.1093/brain/aww015

Palmqvist S, Schöll M, Strandberg O, Mattsson N, Stomrud E, Zetterberg H, Blennow K, Landau S, Jagust W, Hansson O. 2017. Earliest accumulation of β-amyloid occurs within the default-mode network and concurrently affects brain connectivity. *Nat Commun* **8**. doi:10.1038/s41467-017-01150-x

Schindler SE, Bollinger JG, Ovod V, Mawuenyega KG, Li Y, Gordon BA, Holtzman DM, Morris JC, Benzinger TLS, Xiong C, Fagan AM, Bateman RJ. 2019. High-precision plasma β-amyloid 42/40 predicts current and future brain amyloidosis. *Neurology* 10.1212/WNL.0000000000008081. doi:10.1212/wnl.0000000000008081

Schöll M, Lockhart SN, Schonhaut DR, O'Neil JP, Janabi M, Ossenkoppele R, Baker SL,

Vogel JW, Faria J, Schwimmer HD, Rabinovici GD, Jagust WJ. 2016. PET Imaging of Tau Deposition in the Aging Human Brain. *Neuron* **89**:971–982. doi:10.1016/j.neuron.2016.01.028

Shaw LM, Vanderstichele H, Knapik-Czajka M, Clark CM, Aisen PS, Petersen RC, Blennow K, Soares H, Simon A, Lewczuk P, Dean R, Siemers E, Potter W, Lee VM, Trojanowski JQ. 2009. Cerebrospinal fluid biomarker signature in Alzheimer's disease neuroimaging initiative subjects. *Ann Neurol* **65**:403–13. doi:10.1002/ana.21610

Sperling RA, Mormino EC, Schultz AP, Betensky RA, Papp K V., Amariglio RE, Hanseeuw BJ, Buckley R, Chhatwal J, Hedden T, Marshall GA, Quiroz YT, Donovan NJ, Jackson J, Gatchel JR, Rabin JS, Jacobs H, Yang HS, Properzi M, Kirn DR, Rentz DM, Johnson KA. 2019. The impact of amyloid-beta and tau on prospective cognitive decline in older individuals. *Ann Neurol* **85**:181–193. doi:10.1002/ana.25395

Villemagne VL, Burnham S, Bourgeat P, Brown B, Ellis KA, Salvado O, Szoeke C, Macaulay SL, Martins R, Maruff P, Ames D, Rowe CC, Masters CL. 2013. Amyloid β deposition, neurodegeneration, and cognitive decline in sporadic Alzheimer's disease: A prospective cohort study. *Lancet Neurol* **12**:357–367. doi:10.1016/S1474-4422(13)70044-9

Wood SN. 1994. Monotonic smoothing splines fitted by cross validation. *SIAM* **15**:1126–1133. doi:10.1137/0915069

Zetterberg H, Mattsson N. 2014. Understanding the cause of sporadic Alzheimer's disease. *Expert Rev Neurother* **14**:621–630. doi:10.1586/14737175.2014.915740
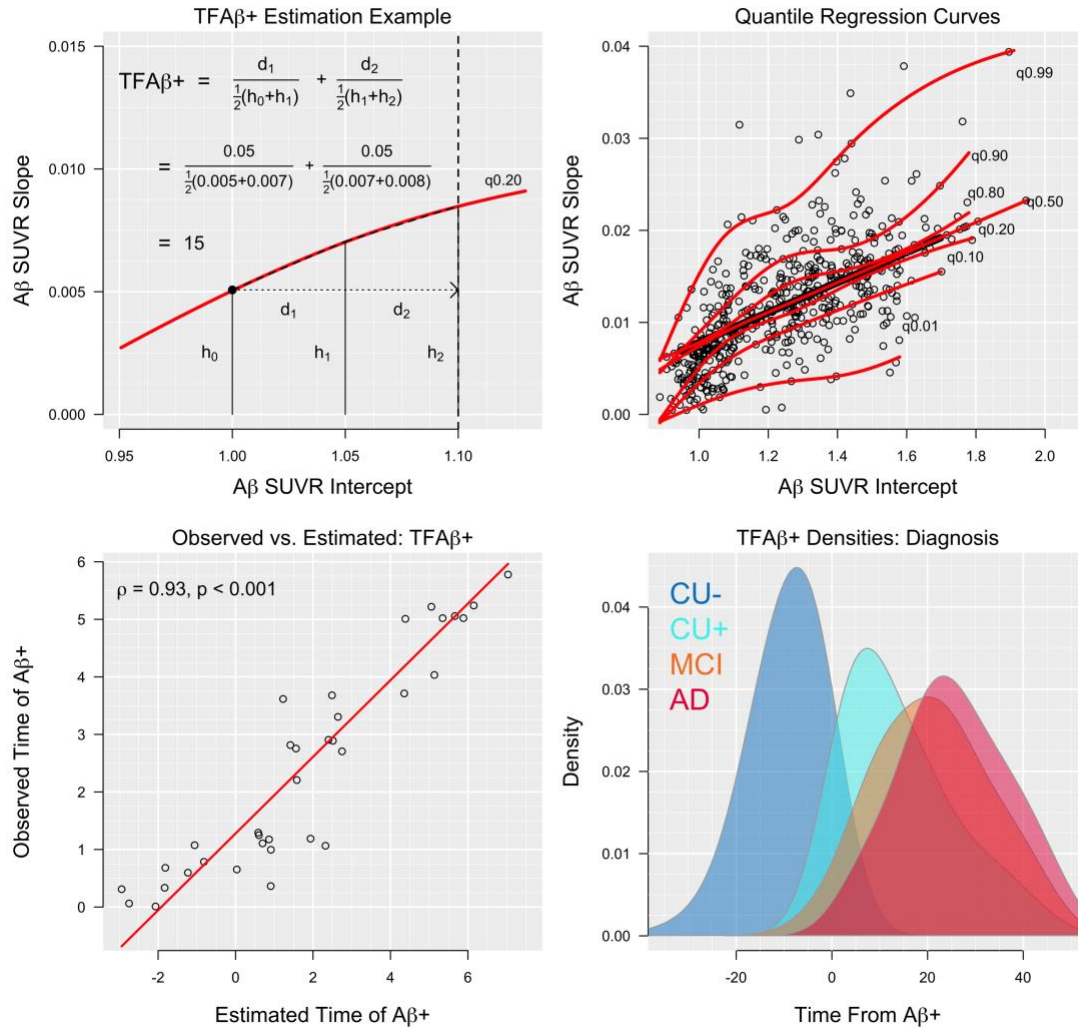
Figures

Figure 1. Observed vs. Estimated TFAβ+, Quantile Regression Curves and TFAβ+ Densities

Top left panel: an example of how TFAβ+ is estimated. Here we have a participant with an estimated intercept of SUVR = 1.00 and an accumulation rate (slope) of 0.005 SUVR/year. We want to calculate how long it will take for them to reach the 1.10 threshold. A slope of 0.005 SUVR/year puts this participant on the 0.20 quantile (20% percentile) curve. We know this participant must accumulate 0.10 SUVR to reach the threshold and we will assume they will continue to have an accumulation rate in the 0.20 quantile. Partitioning the curve into segments from SUVR = 1.00 to 1.10 and using the formula time = distance/rate, the time to cross each segment is calculated and summed. In the figure, only two segments are shown, but in the actual calculation, the curve is partitioned into a large number of segments. Assuming a linear rate increase within each segment (shown in the dashed black line along the red quantile curve), the time to travel the distance in the 1_{st} segment, from SUVR 1.00 to 1.05 is given by, $time_1 = d_1/rate_1$, where d_1 is 0.05 and $rate_1$ is the average rate in segment 1, which is $\frac{1}{2}(h_0+h_1)$, as shown in the panel. A similar calculation is done for segment 2 and the results are summed to give TFAβ+ = 15.

Top right panel: quantile regression curves of Aβ PET slopes plotted against intercepts. Curves for several selected quantiles (0.01, 0.10, …, 0.99) are shown in red.

Bottom left panel: observed time of Aβ+ plotted against estimated time of Aβ+.

Bottom right panel: distributions of TFAβ+ for each group, Aβ- CU (CU-), Aβ+ CU (CU+), MCI, and AD are shown.

Figure 2. Regional Aβ PET
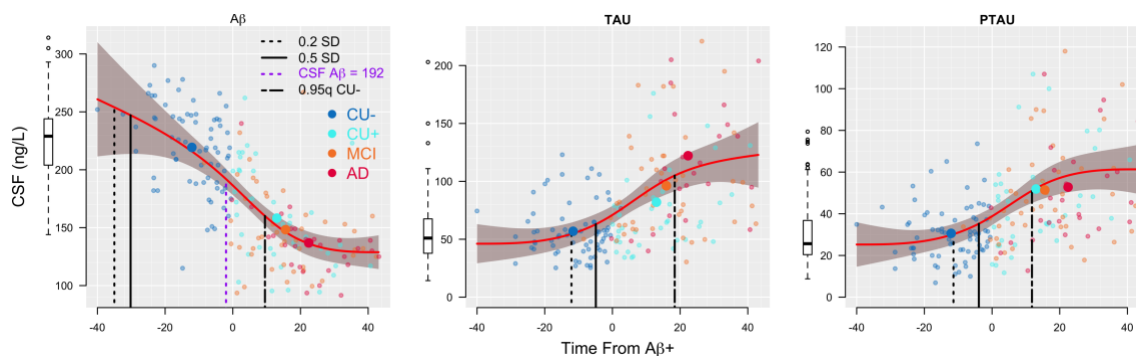
Aβ PET ROIs are plotted against TFAβ+. Effect sizes, depicting change points are shown as vertical dashed (0.2 SD, initial change) and solid (0.5 SD) lines. Regression curves (red) and corresponding 95% CIs (shaded grey) are shown. Mean values of the response are plotted against mean TFAβ+ for each of the four diagnosis groups (large symbols). The 0.95 quantile (approximately 1.65 SD if normally distributed) of the response for the CU- group is also shown (short/long dashed line). The 0.95 quantile (or 0.05 quantile for responses where low values are worse) of the biomarkers in CU-, provided for all responses to facilitate comparisons of when (in terms of TFAβ+) the average level of each response is no longer in the normal range. The boxplots to the left of each figure show the biomarker distribution in subjects that was determined to not be on the AD trajectory (including subjects where the model estimated them to become Aβ+ at over 120 years of age). Effect sizes of Aβ increase are shown in the bottom panel at TFAβ+ = -20, -10, 0, 10, and 20 years.
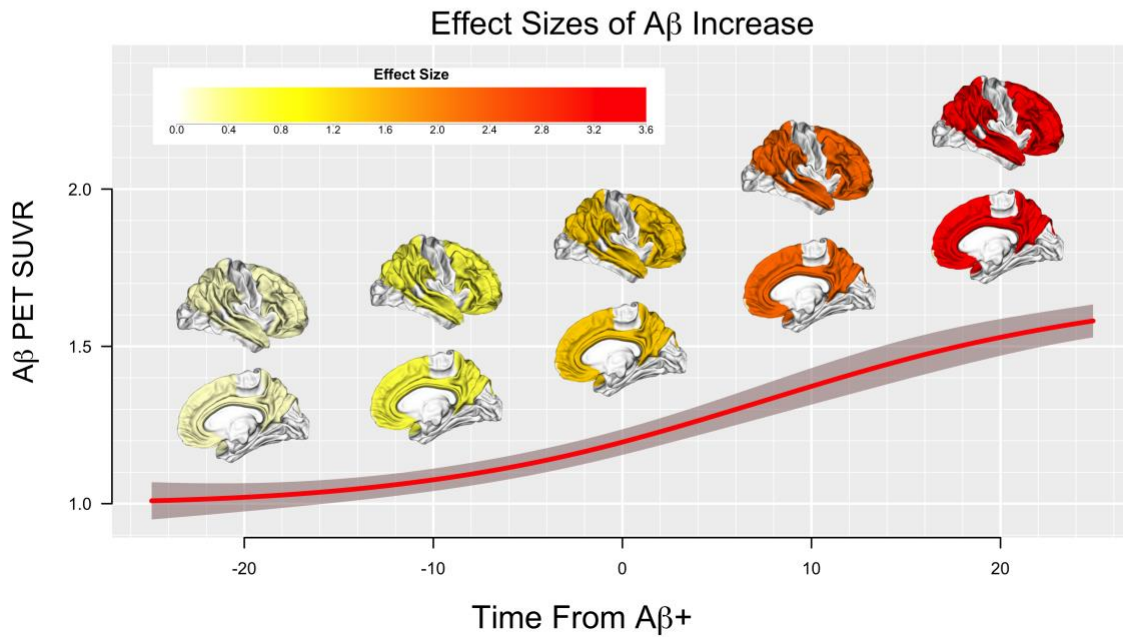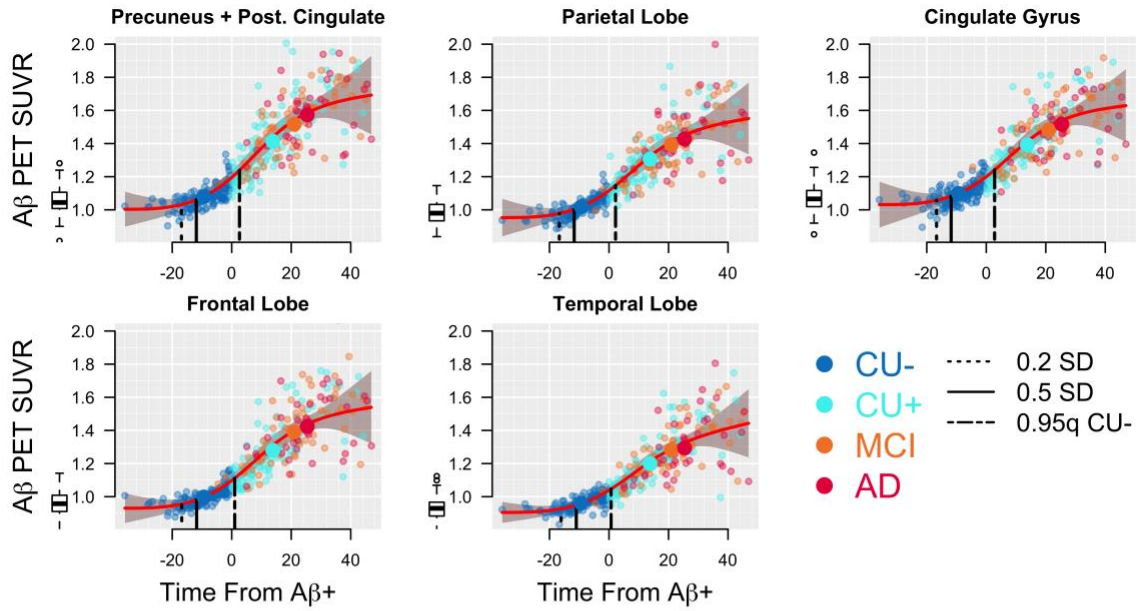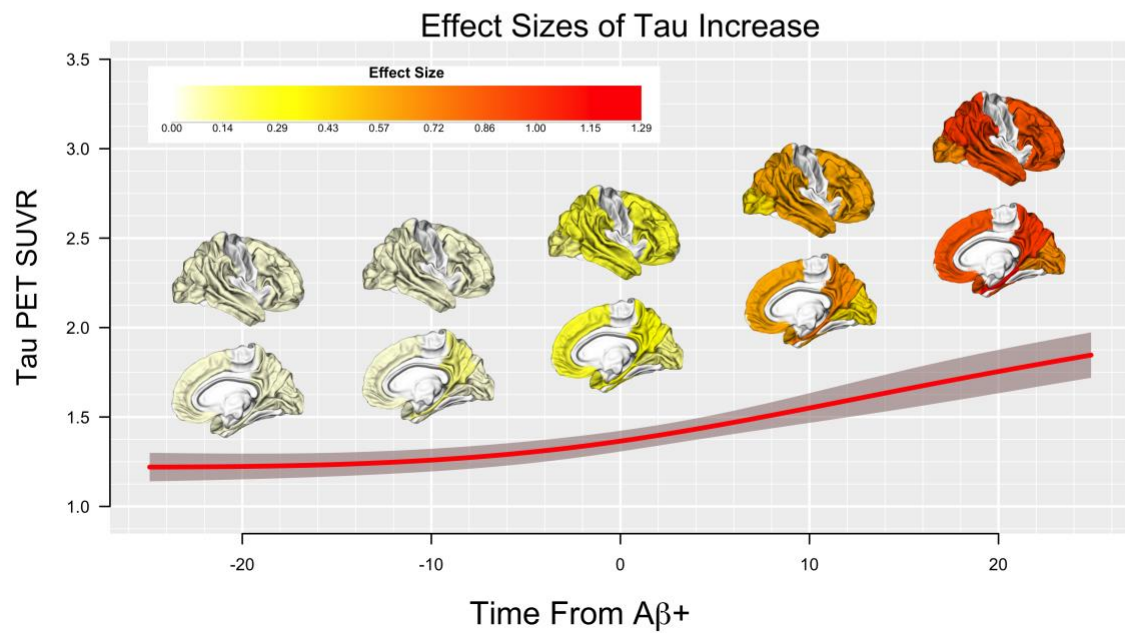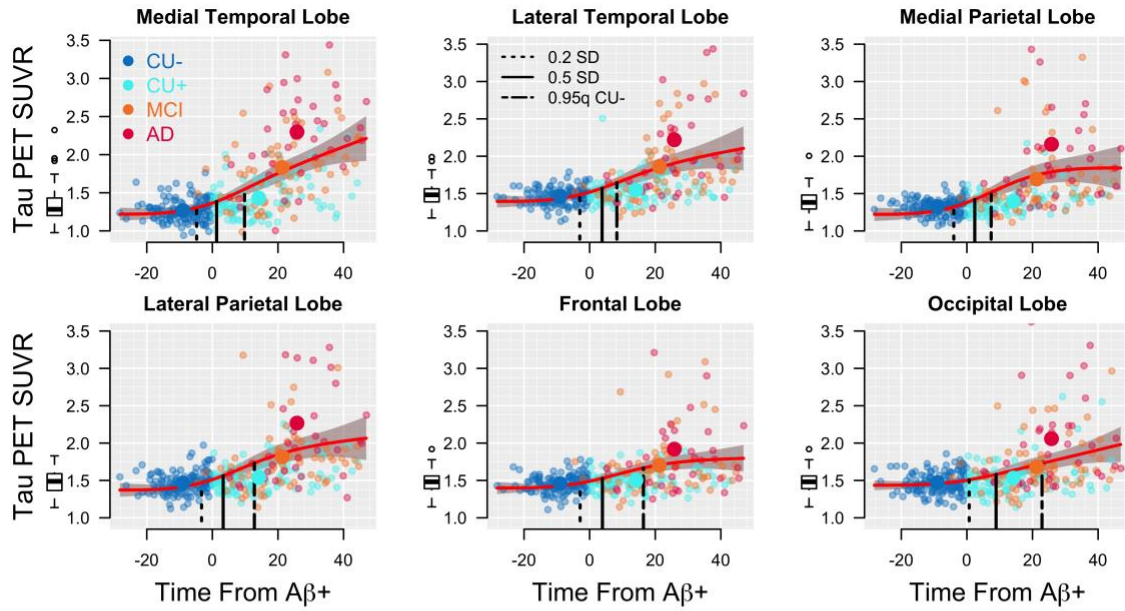
Figure 3. CSF Biomarkers

CSF biomarker responses are plotted against TFAβ+. Effect sizes, depicting change

points are shown as vertical dashed (0.2 SD, initial change) and solid (0.5 SD) lines.

Regression curves (red) and corresponding 95% CIs (shaded grey) are shown. Mean

values of the response are plotted against mean TFAβ+ for each of the four diagnosis

groups (large symbols). The 0.95 quantile (approximately 1.65 SD if normally

distributed) of the response for the CU- group is also shown (short/long dashed line). The

boxplots to the left of each figure show the biomarker distribution in subjects that were

determined not to be on the AD trajectory (including subjects where the model estimated

them to become Aβ+ over 120 years of age).

Figure 4. Regional Tau PET

Tau PET ROIs are plotted against TFAβ+. Effect sizes, depicting change points are

shown as vertical dashed (0.2 SD, initial change) and solid (0.5 SD) lines. Regression

curves (red) and corresponding 95% CIs (shaded grey) are shown. Mean values of the

response are plotted against mean TFAβ+ for each of the four diagnosis groups (large

symbols). The 0.95 quantile (approximately 1.65 SD if normally distributed) of the

response for the CU- group is also shown (short/long dashed line). The boxplots to the

left of each figure show the biomarker distribution in subjects that was determined to not

be on the AD trajectory (including subjects where the model estimated them to become

Aβ+ at over 120 years of age). Effect sizes of tau increase are shown in the bottom panel

at TFAβ+ = -20, -10, 0, 10, and 20 years.

Figure 5. Cognition

MMSE and PACC scores are plotted against TFAβ+. Effect sizes, depicting change points are shown as vertical dashed (0.2 SD, initial change) and solid (0.5 SD) lines. Regression curves (red) and corresponding 95% CIs (shaded grey) are shown. Mean values of the response are plotted against mean TFAβ+ for each of the four diagnosis groups (large symbols). The 0.05 quantile (approximately -1.65 SD if normally distributed) of the response for the CU- group is also shown (short/long dashed line).
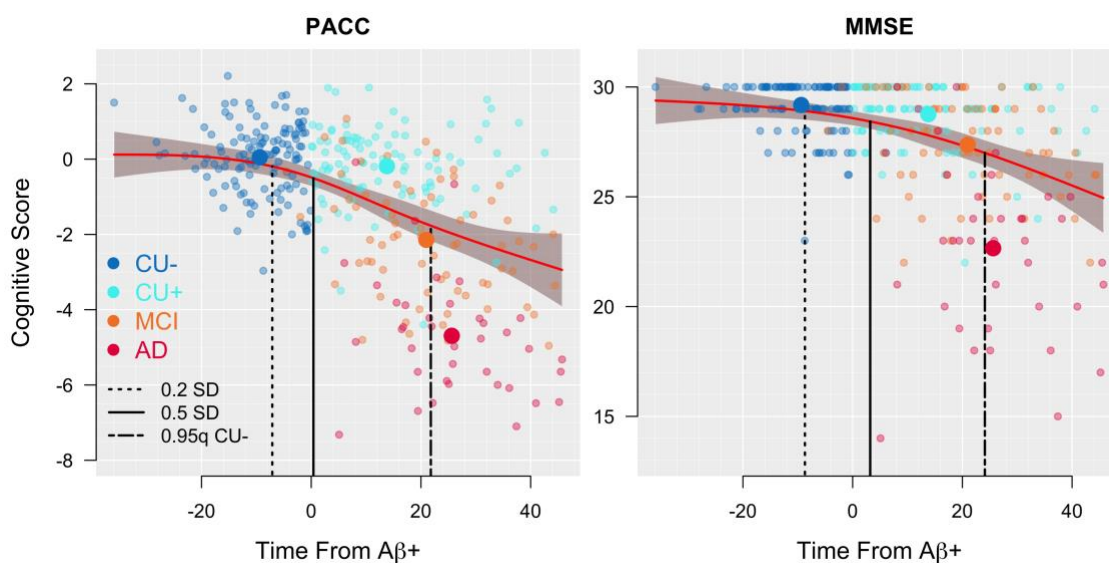
Figure 6. Summary Curves

Summary curves are shown for all modalities on a scale from zero to one. Responses are

scaled such that zero is the least pathological point for each response and one is the mean

response in the AD participants. The initial effect, defined by 0.2 SD change points are
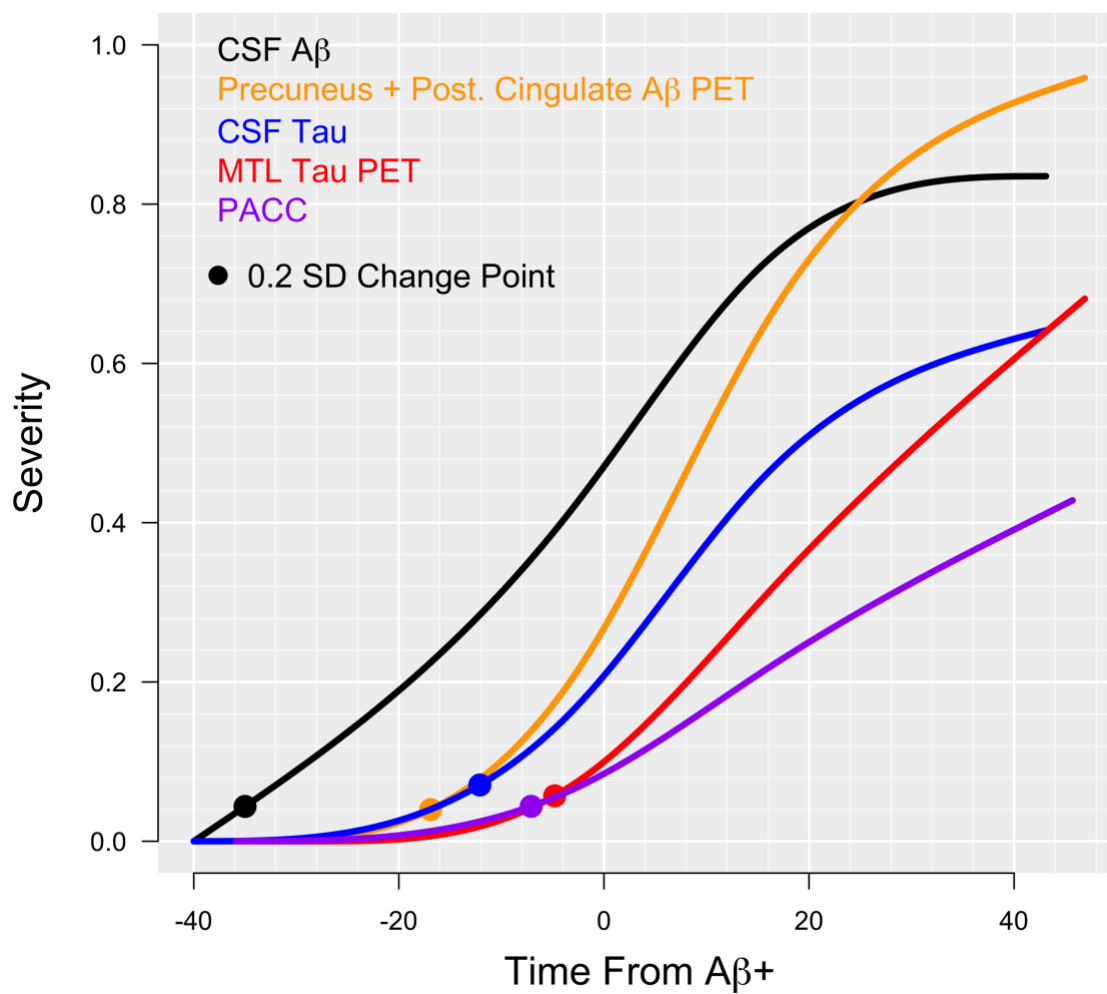
plotted.

Table 1. Initial values, effect sizes and change points

	Initial Value (SD)	Value at TFAβ+ = 0	Difference at TFAβ+ = 0 (p-value)	95% CI	Effect Size (Difference at TFAβ+ = 0)	TFAβ+ Change Point (0.2 SD)
Aβ PET						
Precuneus+PC	1.00 (0.14)	1.20	0.19 (<0.01)	0.09 to 0.30	1.35	-17
Parietal Lobe	0.95 (0.12)	1.12	0.16 (<0.01)	0.06 to 0.27	1.32	-17
Cingulate Gyrus	1.03 (0.13)	1.20	0.17 (0.01)	0.04 to 0.30	1.32	-17
Frontal Lobe	0.93 (0.13)	1.10	0.17 (<0.01)	0.08 to 0.26	1.32	-17
Temporal Lobe	0.91 (0.11)	1.04	0.13 (<0.01)	0.07 to 0.20	1.20	-16
CSF						
Aβ	261 (34)	186	-74 (<0.01)	-123 to -25	-2.17	-35
T-tau	46 (42)	71	25 (0.01)	7 to 43	0.59	-12
P-tau	25 (25)	39	14 (0.02)	2 to 25	0.55	-11
Tau PET						
MPL	1.22 (0.49)	1.38	0.16 (0.02)	0.02 to 0.29	0.32	-4
MTL	1.22 (0.41)	1.37	0.15 (0.02)	0.03 to 0.26	0.35	-5
LTL	1.40 (0.44)	1.52	0.12 (0.05)	0.00 to 0.25	0.28	-3
LPL	1.37 (0.47)	1.51	0.14 (0.04)	0.01 to 0.27	0.29	-3
Frontal Lobe	1.40 (0.33)	1.49	0.09 (0.13)	-0.03 to 0.21	0.28	-3
Occipital Lobe	1.44 (0.36)	1.50	0.07 (0.13)	-0.02 to 0.16	0.19	1
Cognition						
MMSE	29.4 (2.38)	28.6	-0.80 (0.17)	-1.93 to 0.33	-0.34	-9
PACC	0.12 (1.56)	-0.49	-0.61 (0.07)	-1.25 to 0.04	-0.39	-7